Submitted: 01 February 2018

Published online in 'accepted manuscript' format: 19 November 2019

Manuscript title: Coupled CO_2 Sequestration Simulation Using ABAQUS and ECLIPSE

Authors: Qi Li[1,2], Wenbin Fei[3], Jianli Ma[1,2], Miao Jing[1,4], Xiaochen Wei[5]

Affiliations: [1]State Key Laboratory of Geomechanics and Geotechnical Engineering, Institute of Rock and Soil Mechanics (IRSM), Chinese Academy of Sciences, Wuhan 430071, China. [2]University of Chinese Academy of Sciences, Beijing 100049, China. [3]Department of Infrastructure Engineering, The University of Melbourne, Melbourne, Australia. [4]Helmholtz-Zentrum für Umweltforschung (UFZ), 04318 Leipzig, Germany. [5]School of Geoscience and Technology, Southwest Petroleum University, Chengdu 610500, China.

Corresponding author: Qi Li, State Key Laboratory of Geomechanics and Geotechnical Engineering, Institute of Rock and Soil Mechanics (IRSM), Chinese Academy of Sciences, Wuhan 430071, China. Tel.: 0086-27-87198126

E-mail: qli@whrsm.ac.cn

Accepted manuscript
doi: 10.1680/jenge.18.00036

Abstract

Thermo-hydro-geomechanical (THM)-coupled physical problems widely occur in geologic carbon sequestration (GCS), which has gained increasing attention in recent years. There are many in-house and commercial software programs developed for THM-coupled numerical simulation. However, only a few programs permit large-scale, complex analysis and prediction of GCS problems. Therefore, we developed an in-house code named the AEEA Coupler to link two industrial standard simulation software programs, ABAQUS (mechanical engineering) and ECLIPSE (petroleum engineering), which enable the THM simulation of large-scale complex geological model (include multiple fractures and faults) possible. In this paper, we introduced interpolation and adaptive search algorithms and data exchange techniques between different grids using reservoir analysis and finite element mesh methods in a mechanical analysis of a reservoir. After that, the applicability and accuracy of the AEEA Coupler were tested by comparing the results with certain benchmarks. Finally, a complicated problem was identified to demonstrate the power of the AEEA Coupler in solving coupled processes in geoscience projects.

Notation

C	constant compression coefficient
P	pore pressure
P_{ref}	reference pressure
$\bar{P}$	average pore pressure
P_c	capillary pressure
P_{c0}	initial capillary pressure
V_p	pore volume at the pore pressure, P
$V_p(P_{ref})$	pore volume at the reference pressure, P_{ref}
α	Biot's coefficient
ϕ	porosity
ϕ_0	porosity when the effective stress in the rock is zero
ϕ_r	residual porosity at high effective stress
σ_i	stress
σ_i'	effective stress
σ_M'	average effective stress
k	permeability
k_0	initial permeability
t_k, t_{k+1}	kth and $(k+1)$th time step
Δx, Δy, Δz	grid dimensions in three directions

Introduction

Thermo-hydro-mechanical (THM)-coupled physical problems occur in engineering projects such as geologic CO_2 sequestration (GCS), oil and natural gas underground sequestration, deep resource exploitation, high-level radioactive waste disposal, and enhanced geothermal systems, and these problems have gained increasing attention in recent years (Regenauer-Lieb et al., 2013, Fang et al., 2013, Xu et al., 2016, Li et al., 2009). The critical research value of solving these problems, such as ensuring the safety of the engineering design, construction and operation of these projects, has gradually become more prominent. Due to laboratory research limitations, which involve the very complicated coupling of processes related to hydrogeology, geochemistry, thermodynamics and rock mechanics, numerical simulation is usually applied in practice as an economic and effective method that permits large-scale, complex analysis and prediction. In GCS projects, the effects of physical and chemical changes, capacity and penetration ability of reservoirs as well as rock mechanic changes in the sequestration formation and caprock could be obtained by laboratory experiments and numerical simulation (Sarhosis et al., 2016).

THM-coupled problems in reservoir engineering currently are usually simulated by the following coupled methods (Samier et al., 2003, Minkoff et al., 2003):

(1) Constant compression coefficient

The pore volume, which is only related to the pore pressure, is adjusted in the software during numerical simulation using the following equations:

$$V_p(P) = V_p(P_{ref}) \cdot \left(1 + X + \frac{X^2}{2} \right) \quad (1)$$

$$X = C \cdot (P - P_{ref}) \quad (2)$$

where V_p is the pore volume at the pore pressure, P; $V_p(P_{ref})$ is the pore volume at the reference pressure, P_{ref}, and C is the constant compression coefficient.

(2) One-way coupling

(3) The pore pressure field and the temperature field calculated by fluid equations are applied as external loads to the mechanical model, and the results of the mechanical calculation need not be fed back to the fluid calculation. This method converges rapidly and is suitable when only focusing on the mechanics process. In the analysis of the relative displacement of a fault and the stress along the fault, one-way coupling is the most suitable method if the model sizes are the same. The existing simulators developed based on this coupling method are ECLIPSE 300-VISAGE, NUFT-LEDC, and FEHM-ABAQUS. Two-way coupling

The two-way coupling method (Samier et al., 2003) is able to couple the best software programs in fluids and mechanics areas. The fluids software and the mechanics software are run consecutively. Specifically, at a certain time step, the pore pressure and temperature are solved by the fluids software, while the mechanics software is suspended. Then, the fluids software is paused, and the calculated pore pressure and temperature are imported into the mechanics software to update certain parameters (e.g., the porosity) that are required by the fluids software at the next time step.

The improved method also considers the relationship between the porosity,

permeability and water saturation, which reflects the weakening effect due to the pore fluid.

The advantage of the latter approach is that the method is flexible and convenient. If the compression coefficients of the different regions of a reservoir are inconsistent, multiple correlation equations can then be defined accordingly. Furthermore, this two-way coupling method can be used for calculations using complex constitutive equations and geometric models. TOUGH2-FLAC3D, ABAQUS-ECLIPSE, and ATHOS-VISAGE are widely used software programs for this kind of coupling.

(4) Full coupling

In the full coupling method, explicit solutions of all partial differential equations are derived simultaneously. This method uses the same mesh in both the reservoir models and mechanical models, and the finite volume method is usually used in reservoir simulation software as well as mechanical simulation software. However, the full coupling method is still in the development stage and can only be applied in the reservoir and caprock areas without consideration of the impact of the surrounding rock boundary conditions. In addition, the computational complexity and poor convergence of the calculations result in this method only being suitable for relatively simple constitutive equations and geometric models. Popular numerical simulators developed based on the full coupling method are CodeBright, OpenGeoSys, FEHM, Dynaflow, and COMSOL (Li et al., 2009).

Accepted manuscript
doi: 10.1680/jenge.18.00036

However, no existing commercial software and open-source code are available for the functionalities of solving THM coupling and tackling complex geometry. In the latest papers, THM is coupled in COMSOL (e.g., Shi et al., 2019) and in-house code (e.g., Salimzadeh and Nick, 2019; Vilarrasa et al., 2014) can only deal with simplified geometry. In this paper, a program named the AEEA Coupler is developed by linking two industrial simulation software programs, namely, ABAQUS (mechanical engineering) and ECLIPSE (petroleum engineering), which are widely used and highly recognized in their respective fields, using the programming language Python 2.7 (Fei et al., 2015). After linking the two software, the complex non-linear mechanical response can be investigated in ABAQUS, for example, the fracture reactivation and the contact behaviors between wellbores and concretes. Moreover, advanced built-in methods such as smoothed-particles hydrodynamics, cohesive element make better simulation possible. The AEEA Coupler is two-way coupling which enables the THM simulation of large-scale complex geological model (include multiple fractures and faults) possible, and applied for the coupled problems encountered in China's Shenhua GCS demonstration project. The Python language is an object-oriented, dynamic programming language with a very concise and clear syntax that can be used to quickly develop program scripts or develop large-scale software programs, especially for high-level programming tasks (Fei et al., 2014). Accessing the ABAQUS results database with Python scripts is one of the most frequently used features with obvious advantages. The Python language is used since it supports the secondary development of ABAQUS with the capability to directly call individual modules in ABAQUS, which can greatly improve the efficiency of software operation. The AEEA Coupler is specific

to the aforementioned tools, ECLIPSE and ABAQUS, but can be easily expanded to other tools.

In this paper, after the development of the AEEA Coupler, the applicability and accuracy were tested by comparing the results with certain benchmarks. Then, a case of wellbore mechanics was designed to present the flexibility of the AEEA Coupler when simulating various different computational grids. Finally, some concluding remarks are provided.

Coupling mechanism of the AEEA Coupler

When two software programs, i.e., ABAQUS and ECLIPSE, are linked together, i.e., coupled, the total simulation time is divided into several steps according to the calculation precision and the computer efficiency. The software programs perform calculations individually, and the parameters are transferred to each other at each time step. The effect of the effective stress on the porosity and permeability of rock as well as the effect of the fluid pressure and temperature on rock deformation are considered in the coupling equation.

As shown in Fig. 1, a multiphase thermo-hydraulic (TH) or thermo-hydro-chemical (THC) coupling operation is first performed by ECLIPSE (Kuang et al., 2014), and then, the center point position and the temperature, pore pressure and saturation information of the ECLIPSE difference grid are read by the bridging program, the AEEA Coupler. Meanwhile, the distribution of the temperature and pore pressure of the corresponding ABAQUS finite element mesh are calculated. Afterwards, ABAQUS starts the THM-coupled analysis (Li et al., 2006), and then, the integral point position and stress information of the ABAQUS finite element mesh are read by the AEEA Coupler. Thereafter, the porosity, permeability and capillary

pressure under the influence of stress are calculated and transferred to the corresponding difference grid of ECLIPSE by the AEEA Coupler. Regarding the role of the water retention behavior, the default relationship is used in ABAQUS. The relationships among the porosity, permeability and stress are established in the mechanics software. The relationships depend on the constitutive model selected in the mechanics software.

The entire THM analysis consists of sequential explicit coupling, and the analysis steps are depicted in Fig. 2. The TH(C)-coupled analysis is conducted first by ECLIPSE from time step t_k to t_{k+1}, and the obtained result is transmitted to ABAQUS at time step t_k. Then, the THM-coupled analysis is performed by ABAQUS from time step t_k to t_{k+1}, and the result is fed back to ECLIPSE at time step t_{k+1}, so that the next time step of the analysis and calculation can be performed by ECLIPSE afterwards.

In an isotropic rock mass, the porosity and permeability have a certain relationship with the average effective stress of the rock mass. A dynamic adjustment is conducted over the whole time of the numerical simulation. The relationship between the porosity, ϕ, and average effective stress, σ'_M, (Davies and Davies, 2001), is addressed as follows:

$$\phi = (\phi_0 - \phi_r) \cdot \exp(5 \cdot 10^{-8} \cdot \sigma'_M) + \phi_r \tag{3}$$

where ϕ_0 is the porosity when the effective stress in the rock is zero and ϕ_r is the residual porosity at high effective stress, and the two parameters can be determined by laboratory experiments. The average effective stress of the rock mass can be obtained from the following equation:

$$\sigma'_M = \frac{1}{3}(\sigma'_1 + \sigma'_2 + \sigma'_3) \tag{4}$$

The effective stress, σ_i', is calculated by equation (5) when the tensile stress is positive.

$$\sigma_i^{'} = (\sigma_i + \alpha \bar{P}) \qquad \text{i=1, 2, 3} \tag{5}$$

where α is the Biot's coefficient (Biot, 1941), σ_i is the stress, and $\bar{P}$ is the average pore pressure that can be calculated by the following equation (Rutqvist et al. 2002):

$$\bar{P} = S_l P_l + (1 - S_l) P_g \tag{6}$$

where *S* is the saturation, *P* is the pressure, and the subscripts *l* and *g* indicate liquid and gas, respectively.

The relationship between the permeability and porosity is an exponential equation and is as follows (Davies and Davies, 2001):

$$k = k_0 \exp[22.2(\phi / \phi_0 - 1)] \tag{7}$$

Meanwhile, the capillary pressure is calculated (Leverett, 1941) by:

$$P_c = P_{c0} \sqrt{\frac{k_0 \times \phi}{k \times \phi_0}} \tag{8}$$

where k is the permeability, k_0 is the initial permeability, P_c is the capillary pressure, and P_{c0} is the initial capillary pressure. This equation is adopted with the aim of updating the capillary pressure by the stress (i.e., the capillary pressure is indirectly dependent on the mean stress). The same equation is also used to couple FLAC and TOUGH2 (Rutqvist et al, 2002).

ABAQUS is a software that was developed based on the finite element method, while ECLIPSE is a software that was developed based on the finite difference method, which means that the computational grids are different between the two software programs. In ABAQUS, the force is loaded on a node, and the data are output at the integration point. In ECLIPSE, each

Accepted manuscript
doi: 10.1680/jenge.18.00036

grid has properties only at the center point, and the coordinates of each grid are determined by the corner points. As shown in Fig. 3, the data at each center point of the grid in ECLIPSE are transmitted to a node in ABAQUS while calculating, and then, the data obtained at an integration point in ABAQUS are transferred to a center point in ECLIPSE.

Capasso and Mantica (2006) first introduced the differential grid when dealing with finite element mesh and finite difference mesh and then removed certain nodes as needed and exchanged the remaining nodes into a finite element mesh. According to this method, the data in the differential grid can be directly used. However, the number of nodes and the shape of meshes are different between the finite element model and the finite difference model, which suggests that this method is not applicable when the region of the finite element mesh is only a part of the area represented by the finite difference mesh. Dean et al. (2006) used the same grid to perform finite element and finite difference analyses, and this technique is quite simple but cannot be used as a general method.

The developed AEEA Coupler program is capable of transforming data between two different grids rapidly, accurately and flexibly even though the size, shape and mesh density are different. Thus, the numerical analysis could be more flexible, and the computational efficiency could be greatly improved.

When two different grids are used for a coupled process analysis, an adaptive search algorithm is adopted for data transmission. The assignment will be made directly if the coordinates of the nodes of the finite element mesh and the center points of the finite difference mesh are coincident. Otherwise, a spherical region search will proceed, as shown in Fig. 4. The

initial search radius is determined by the size of the grid. If the search result does not meet the requirement, the radius size will be changed, and the search will be conducted again. If the search is performed too many times, the search conditions will be appropriately eased.

The inverse distance weighted interpolation (also known as "inverse distance weighted average" or "Shepard method") is used when interpolating the value of the searched point to the node of another grid.

Zhang (2012) used the Shepard method for the digital elevation model, and a significance analysis of the interpolation parameters was performed. The results are addressed as follows:

(1) In terms of the search direction, the four-way search and the eight-direction search do not improve the interpolation precision.

(2) Using 8 to 12 search points is a better choice.

(3) When the weighted index is greater or equal to 3, the effect of the interpolation precision is not clear. A weighted index of 2 or 3 is better.

(4) Based on the significance analysis, the impacts of the three factors mentioned above on the interpolation precision are sorted as "weighted index > number of search points > search direction".

The calculation flow chart of the AEEA Coupler is shown in Fig. 5.

Model validation

Benchmark SPE 79709

This section shows the accuracy of the AEEA Coupler by comparing its results with a standard example proposed by the Society of Petroleum Engineers (SPE) (Dean et al., 2006). The two

problems defined in SPE 79709 are simple single-phase depletion problems that illustrate the role that stress and displacement boundary conditions play in porous flow calculations. Biot's parameters α and 1/M are set equal to 1 and 0, respectively. Problems 1 and 2 are identical in their description except that problem 1 enforces zero displacement boundary conditions at the vertical faces of the grid, and problem 2 applies constant horizontal stresses at the vertical faces of the grid. Fig. 6 shows the stress and displacement boundary conditions for the two problems.

The grid dimensions are 11×11×10 with $\Delta x=\Delta y=60.96$ m in the horizontal direction and $\Delta z=6.096$ m in the vertical direction. The top of the reservoir is at a depth of 1828.8 m, the initial in situ reservoir porosity is 0.2, the residual porosity is 0.19, and the reservoir permeabilities are 50 and 5 mD in the horizontal and vertical direction, respectively. The fluid is a single phase fluid with a formation volume factor of 1.0, a viscosity of 10^{-3} Pa·s, and a fluid density of 999.648 kg/m^3. The initial fluid pressure is 20.68 MPa at a depth of 1828.8 m, and the hydraulic gradient is 9794.71 Pa/m.

The elastic modulus is 68.95 MPa, Poisson's ratio is 0.3, and initial in situ solid density (the solid material without pores) is 2700 kg/m^3. The initial horizontal stress is 27.58 MPa over the entire reservoir depth, while the initial vertical stress gradient is 23143 Pa/m throughout the reservoir. The bottom of the grid has a zero vertical displacement constraint, and all faces of the grid have zero tangential stresses. Both problems apply a normal stress of 41.37 MPa at the top of the grid, while problem 1 enforces zero normal displacements at the four vertical faces

of the grid. Problem 2 applies a normal stress of 27.58 MPa at these same faces. Uniaxial strain behavior is assumed for problem 1, and a constant total stress is assumed for problem 2.

A vertical well with a wellbore radius of 0.0762 m is completed in the center of the reservoir and penetrates all ten layers of the grid, namely, cells (6, 6, 1-10). The well is produced at a rate of 2384.7 m^3/day for 500 days with a time step of 10 days. No flow boundary conditions are assumed for the fluid at all faces of the grid.

Fig. 7 shows how the geomechanical stress or displacement boundary conditions influence the pressure response in the reservoir, and Fig. 8 shows the subsidence at the top of the reservoir at the well for problems 1 and 2. The results obtained by the AEEA Coupler were compared with the benchmark example of SPE 79709, as shown in Figs. 7 and 8. Due to the different code programming principles of the two software programs and the constant fluid compressibility used in the SPE 79709, there was a slight deviation. In the case of the boundary constraints in Fig. 7, the fluid compressibility decreased at the later stage when using the AEEA Coupler, which increased the production difficulty. Therefore, the average pore pressure at the later stage was slightly higher than the value obtained in the benchmark example. Fig. 8 shows that the subsidence at the early stage was larger than that in the benchmark example, which was also due to the decreasing porosity and permeability obtained by the AEEA Coupler during the analysis.

Benchmark SPE 125760

The benchmark validation model of SPE 125760 in this section has been widely used by Cuisiat et al. (1998), Dean et al. (2006), Samier and GENNARO (2007), and Inoue and da

Fontoura (2009). This section shows the accuracy of the AEEA Coupler by comparison of the results with the work of Inoue and da Fontoura (2009). The model (Fig. 9) contains not only the reservoir but also the surrounding rock for the accuracy of the mechanical boundaries.

The finite difference grid and finite element mesh were made coincident in this model. A mesh of 21×21×12 elements that was called a coarse grid and a mesh of 33×33×17 elements that was called a fine grid were used by Inoue and da Fontoura (2009). Furthermore, a comparison between the full coupling and two-way coupling method results was made as well. The results indicate that the precision was higher in the fine grid, which needs a large amount of computation. Only 7 seconds were needed in the coarse grid for each mechanical calculation, while the fine grid needs 47 seconds. Moreover, a significant difference between the results of the two-way coupling method and the full coupling method in a coarse grid was still acceptable if the precision requirement was not high.

To verify that the developed AEEA Coupler could still be used with a coarse grid, a grid of 21×21×12 elements was adopted in this study. The grid model is shown in Fig. 10, and the material parameters used in the simulation are listed in Table 1.

The vertical stress gradient in the z-direction was 22.62 kPa/m with an initial vertical stress of 0 MPa at the surface, and the initial horizontal stresses were equal to half of the vertical stress. The boundary conditions at the side and bottom of the finite element mesh had zero normal displacement. A vertical well with a wellbore radius of 0.0762 m and a production rate of 0.092 m^3/s was completed in all layers in the center of the reservoir. The analysis was performed for a time period of 2000 days. The results and comparison are shown in Figs. 11-13.

Compared with SPE 125760, the average pore pressure decreased to 27.45 MPa after 2000 days, and the result of the AEEA Coupler was 27.39 MPa. After 2000 days, the compaction at the top of the reservoir and the surface subsidence calculated by SPE 125760 were -1.434 m and -0.663 m, respectively, while the results of AEEA Coupler were -1.493 m and -0.69 m, respectively. The slight deviation in the computational results was caused by the different code programming principles of the software used.

Mechanical analysis of the wellbore

In a GCS project, a safety analysis of the wellbore is of vital importance. Different software programs have different processing techniques for the simulation of a wellbore. The AEEA Coupler can use different grids in both ABAQUS and ECLIPSE to flexibly analyze the wellbore performance. In particular, by using solid elements for the wellbore, different contact modes can be accomplished between the wellbore and the formation in the AEEA Coupler. This flexibility leads to a more realistic result compared with the projected wellbore path method widely used in reservoir simulations (Bostrøm and Skomedal, 2004). The model with the grid is shown in Fig. 14.

The geometric model was 3000 m high, 4400 m long and 4400 m wide. A 2 m thick reservoir was buried at a depth of 1638 m. A vertical injection well, with an outer diameter of 0.09 m and a wall thickness of 0.01 m injecting CO_2 at a fixed pressure of 25 MPa, was completed in the center of the reservoir. Only hydromechanical coupling was considered in the reservoir, and the solid element type of the reservoir and surrounding rock was C3D8P and C3D8R, respectively. The analysis was performed for a time of 2 years. In addition, the

properties of the material are given in Table 2.

Fig. 15 shows the pore pressure distribution at the top of the reservoir. After 1 year of injection, the pore pressure at the reservoir boundary increased to 17.47 MPa after 1 year and 17.91 MPa after 2 years.

Fig. 16 shows that the injection point and the reservoir boundary were uplifted by 0.731 and 0.0468 mm, respectively, after 1 year and the uplift increased to 0.772 and 0.118 mm after 2 years, respectively.

Fig. 17 shows the vertical displacement of the wellbore. The injection of CO_2 caused the wellbore above the reservoir to rise, and the largest uplift occurred at the bottom of the caprock, which was 0.73 mm after 1 year and 0.77 mm after 2 years.

According to the above performance analysis of the wellbore, as the pressure diffused around the reservoir, the displacement changed more at the boundary. For the purpose of monitoring, attention should be paid to monitoring near the injection well during the first few days of injection. If there are faults in the reservoir far away from the injection well, it is necessary to pay attention to activation of the faults for long-term monitoring.

Conclusions

Numerical simulation has been an important method to study and analyze THM-coupled problems in recent years. Based on the coupling theory of multiphysics, the AEEA Coupler was developed and verified by comparison with benchmarks to ensure its accuracy and applicability. An example of wellbore mechanics has also been designed to demonstrate the flexibility of the AEEA Coupler when performing simulations between various computational

grids. The applied cases in this paper are relatively simple. Complex faults and geochemical processes have not yet been considered. How to use the AEEA Coupler in a model associated with fault reactivation is still a subject that needs further research.

The main conclusions are addressed as follows:

(1) The AEEA Coupler is not only suitable for GCS engineering but can also be applied to the underground storage of oil and gas, exploitation of coalbed methane and shale gas and other unconventional deep mining projects. This bridging software can be directly called using the Python language. Furthermore, the inverse distance weighted interpolation algorithm is used to greatly enhance the speed of operation by making contributions to the calculation and data transmission between two different sets of grids in ABAQUS and ECLIPSE.

(2) The verification by benchmarks SPE79709 and SPE125760 was conducted to illustrate the accuracy and applicability of the AEEA Coupler. The reservoir pressure and displacement distribution obtained under different boundary conditions are within acceptable limits.

(3) To illustrate the flexibility of data transmission between the different shapes of the finite difference grid and finite element mesh, this paper analyzed the stability of a CO_2 injection wellbore. The pore pressure, displacement of the reservoir and vertical displacement of the wellbore were investigated during the CO_2 injection process, which provides some references for GCS engineering.

Acknowledgements

The authors acknowledge the financial support from the National Natural Science Foundation of China (NSFC) under grant nos. 41872210 and 41274111.

References

Biot MA (1941) General theory of three-dimensional consolidation. *Journal of Applied Physics* **12(2)**:155-164.

Bostrøm B and Skomedal E (2004) Reservoir geomechanics with ABAQUS. In *Proc. 2004 ABAQUS Users' Conference, Boston, USA*. pp. 117-131.

Capasso G and Mantica S (2006) Numerical simulation of compaction and subsidence using ABAQUS. In *Proc. 2006 ABAQUS Users' Conference, Boston, USA*. pp. 125-144.

Cuisiat F, Gutierrez M, Lewis RW and Masters I (1998) Petroleum reservoir simulation coupling flow and deformation. In *Proc. European Petroleum Conference, The Hague, Netherlands*. 1998, SPE. https://doi.org/10.2118/50636-MS

Davies JP and Davies DK (2001) Stress-dependent permeability: Characterization and modeling. *SPE Journal* **6(2)**:224-235.

Dean RH, Gai X, Stone CM and Minkoff SE (2006) A comparison of techniques for coupling porous flow and geomechanics. *SPE Journal* **11(1)**:132-140.

Fang Y, Nguyen BN, Carroll K, Xu Z, Yabusaki SB, Scheibe TD and Bonneville A (2013) Development of a coupled thermo-hydro-mechanical model in discontinuous media for carbon sequestration. *International Journal of Rock Mechanics and Mining Sciences* **62**:138-147.

Fei W, Li Q, Liu X, Wei X, Jing M, Song R, Li X and Wang Y (2014) Coupled analysis for interaction of coal mining and CO_2 geological storage in Ordos basin, China In *Proceedings of ARMS8 - 2014 ISRM International Symposium - 8th Asian Rock*

Mechanics Symposium - Rock Mechanics for Global Issues - Natural Disasters, Environment and Energy - (Shimizu N, Kaneko K, andKodama J-I (eds)). ISRM Digital Library, Tokyo, pp. 2485-2494.

Fei W, Li Q, Wei X, Song R, Jing M and Li X (2015) Interaction analysis for CO_2 geological storage and underground coal mining in Ordos basin, China. *Engineering Geology* **196**:194-209.

Inoue N and Da Fontoura SA (2009) Answers to some questions about the coupling between fluid flow and rock deformation in oil reservoirs. In *Proc. SPE/EAGE Reservoir Characterization & Simulation Conference, Abu Dhabi, UAE*. https://doi.org/10.2118/125760-MS

Kuang D-Q, Li Q, Wang Y-S, Wang X-J, Lin Q, Wei X-C and Song R-R (2014) Numerical simulation of distribution of migration of CO_2 in Shenhua carbon capture and storage demonstration project. *Rock and Soil Mechanics* **35(9)**:2623-2633, 2641.

Leverett M (1941) Capillary behavior in porous solids. *Transactions of the AIME* **142(01)**:152-169.

Li Q, Ito K, Fu B-H, Sato I, Lei X-L, Okuyama S, Sasai T, Wu ZS, Kazahaya K and Shi B (2009) Coupling and fusion in modern geosciences. *Data Science Journal* **8**:S45-S50.

Li Q, Ito K, Wu ZS, Lowry CS and Loheide II SP (2009) COMSOL Multiphysics: A Novel Approach to Groundwater Modeling. *Ground Water* **47(4)**:480-487.

Li Q, Wu ZS, Bai YL, Yin XC and Li XC (2006) Thermo-hydro-mechanical modeling of CO_2 sequestration system around fault environment. *Pure and Applied Geophysics*

163(11-12):2585-2593.

Minkoff SE, Stone CM, Bryant S, Peszynska M and Wheeler MF (2003) Coupled fluid flow and geomechanical deformation modeling. *Journal of Petroleum Science and Engineering* **38(1-2)**:37-56.

Regenauer-Lieb K, Veveakis M, Poulet T, Wellmann F, Karrech A, Liu J, Hauser J, Schrank C, Gaede O and Trefry M (2013) Multiscale coupling and multiphysics approaches in earth sciences: Theory. *Journal of Coupled Systems and Multiscale Dynamics* **1(1)**:49-73.

Rutqvist J, Wu YS, Tsang CF and Bodvarsson G (2002) A modeling approach for analysis of coupled multiphase fluid flow, heat transfer, and deformation in fractured porous rock. *International Journal of Rock Mechanics and Mining Sciences* **39(4)**: 429-442.

Salimzadeh S and Nick H (2019) A coupled model for reactive flow through deformable fractures in Enhanced Geothermal Systems. *Geothermics* **81**: 88-100.

Samier P and Gennaro SD (2007) A practical iterative scheme for coupling geomechanics with reservoir simulation. In *Proc. EUROPEC/EAGE Conference and Exhibition, London, UK.* SPE. https://doi.org/10.2118/107077-MS

Samier P, Onaisi A and Fontaine G (2003) Coupled analysis of geomechanics and fluid flow in reservoir simulation. In *Proc. SPE Reservoir Simulation Symposium, Houston, Texas, USA*. 2003, SPE. https://doi.org/10.2118/79698-MS

Sarhosis V, Hosking LJ and Thomas HR (2018) Carbon sequestration potential of the South Wales Coalfield. *Environmental Geotechnics* **5(4)**:234-246 https://doi.org/10.1680/jenge.16.00007

Shi Y, Song X, Li J, Wang G, Zheng R and YuLong F (2019) Numerical investigation on heat extraction performance of a multilateral-well enhanced geothermal system with a discrete fracture network. *Fuel* **244**: 207-226.

Vilarrasa V, Olivella S, Carrera J and Rutqvist J (2014) Long term impacts of cold CO_2 injection on the caprock integrity. *International Journal of Greenhouse Gas Control* **24**:1-13.

Xu C, Dowd P and Li Q (2016) Carbon sequestration potential of the Habanero reservoir when carbon dioxide is used as the heat exchange fluid. *Journal of Rock Mechanics and Geotechnical Engineering* **8(1)**:50-59.

Zhang J (2012) Research on adaptability of DEM interpolation method. PLA Information Engineering University, Zhengzhou.

Accepted manuscript
doi: 10.1680/jenge.18.00036

Table 1. The properties of the fluid and formation

Fluid flow	Values	Geomechanics	Values
Viscosity (Pa·s)	10^{-3}	Young's modulus of the surrounding rock (MPa)	6894.8
Fluid density at 0.1013 MPa (kg/m^3)	10^3		
Horizontal permeability (mD)	98.6	Young's modulus of the reservoir (MPa)	68.95
Vertical permeability (mD)	9.86		
Porosity (-)	0.25	Poisson's ratio (-)	0.25
Residual porosity (-)	0.24		

Accepted manuscript
doi: 10.1680/jenge.18.00036

Table 2. The properties of the material

Material	Density (kg/m^3)	Young's modulus (GPa)	Poisson's ratio (-)	Permeability (mD)	Porosity (-)
Rock	2380	9	0.32	10	0.1
Steel	7850	290	0.28		

Accepted manuscript
doi: 10.1680/jenge.18.00036

Figure 1. Schematic of the AEEA Coupler

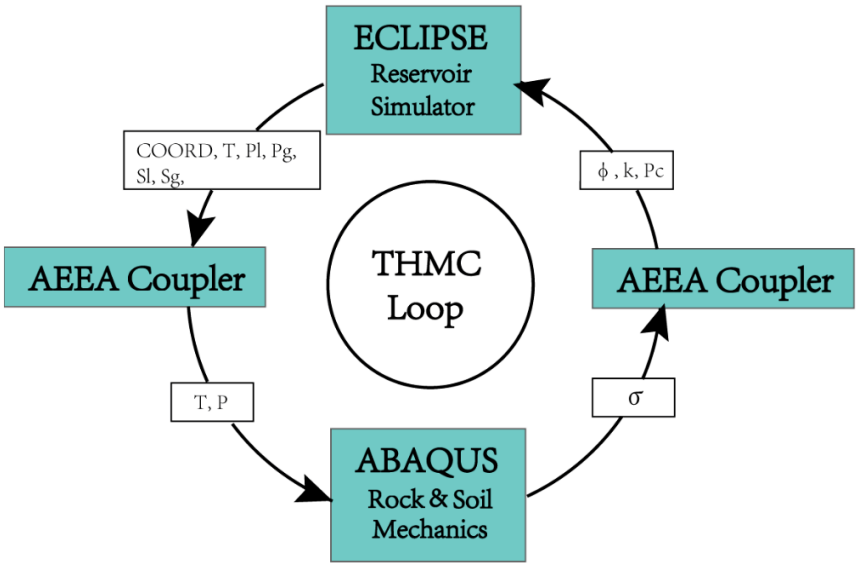

Accepted manuscript
doi: 10.1680/jenge.18.00036

Figure 2. Coupled analysis steps over time

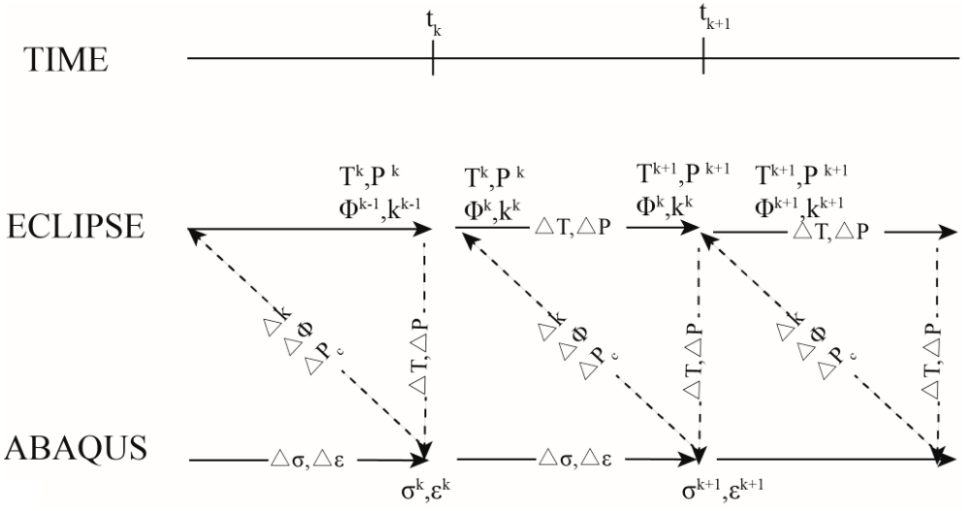

Accepted manuscript
doi: 10.1680/jenge.18.00036

Figure 3. Grid and data transmission points between ABAQUS and ECLIPSE

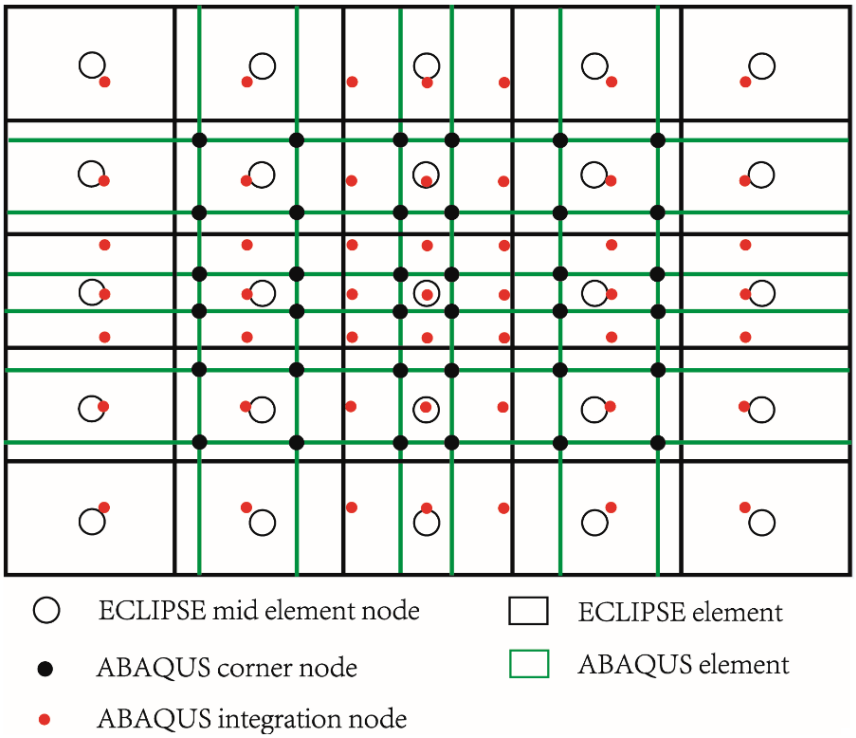

Accepted manuscript
doi: 10.1680/jenge.18.00036

Figure 4. A diagram of the search method

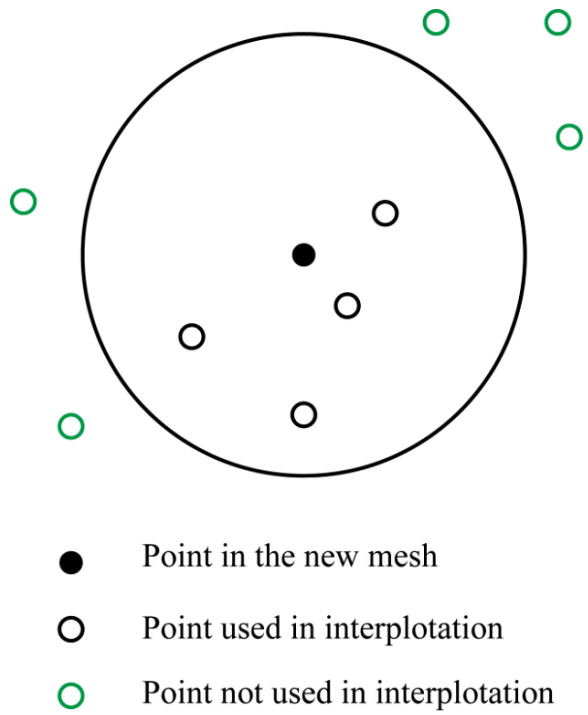

Accepted manuscript
doi: 10.1680/jenge.18.00036

Figure 5. The calculation flow chart of the AEEA Coupler

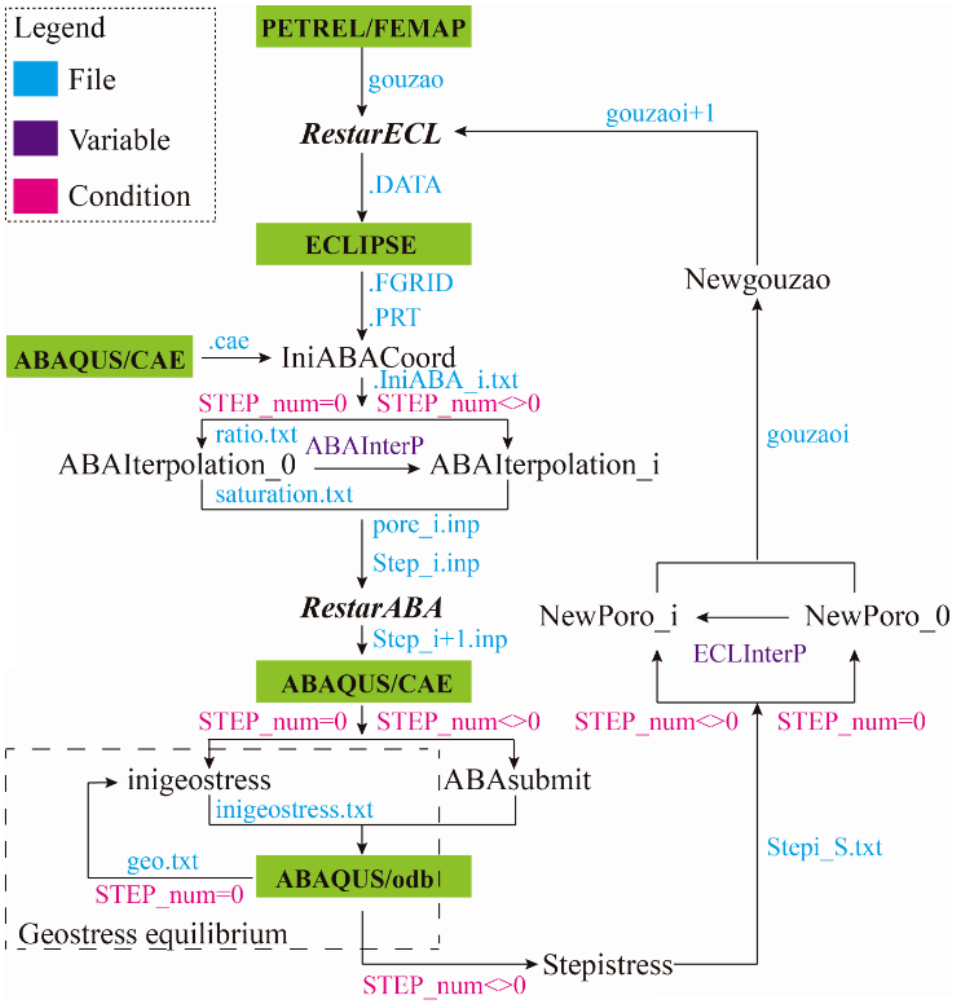

Figure 6. (A) Constrained displacement for problem 1. (B) Unconstrained displacement for problem 2 of SPE 79709

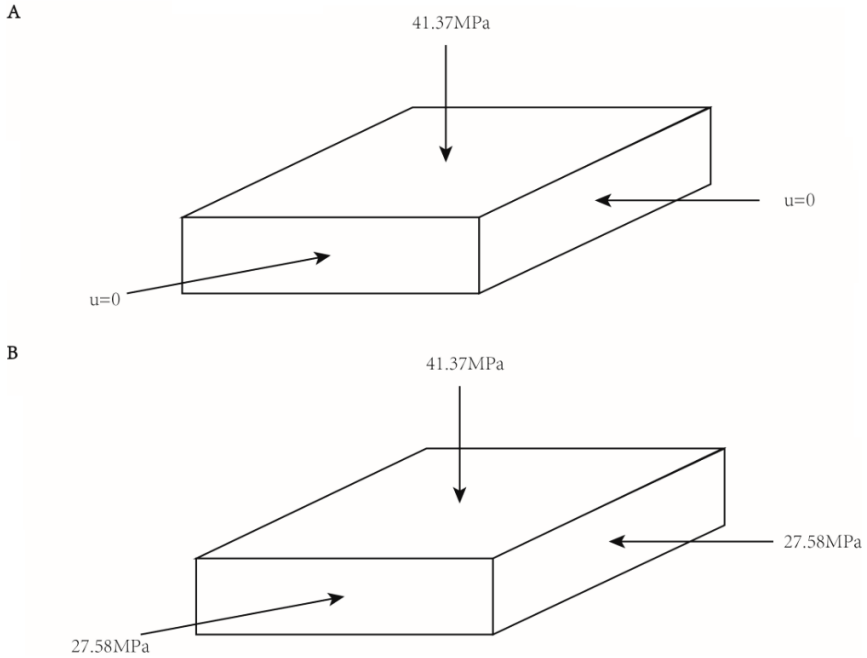

Accepted manuscript
doi: 10.1680/jenge.18.00036

Figure 7. Average pore pressure

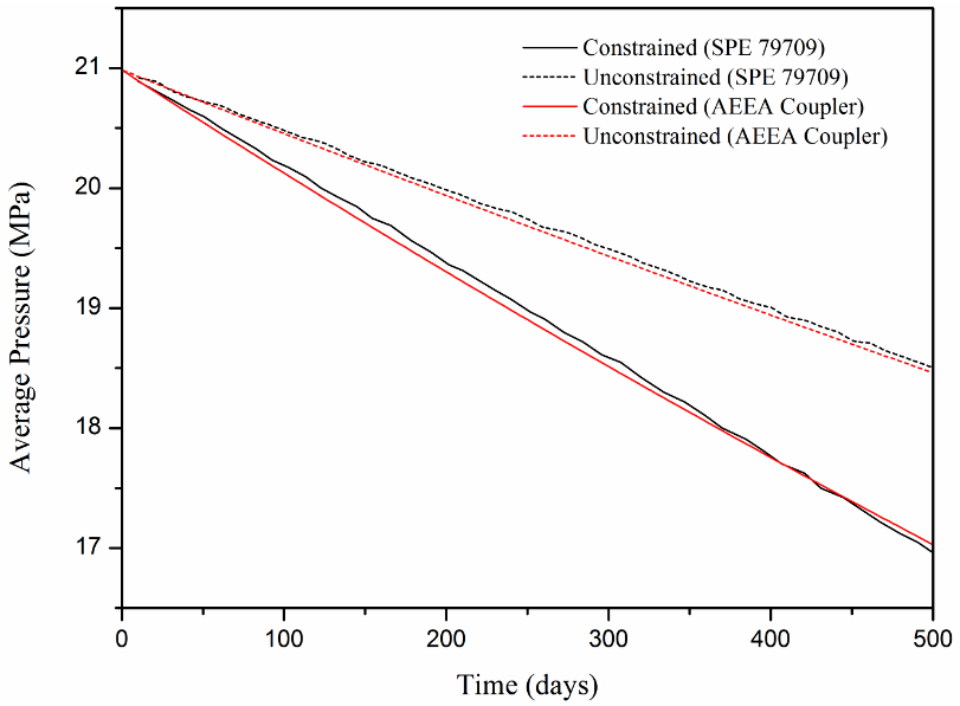

Accepted manuscript
doi: 10.1680/jenge.18.00036

Figure 8. Subsidence at the top of the reservoir

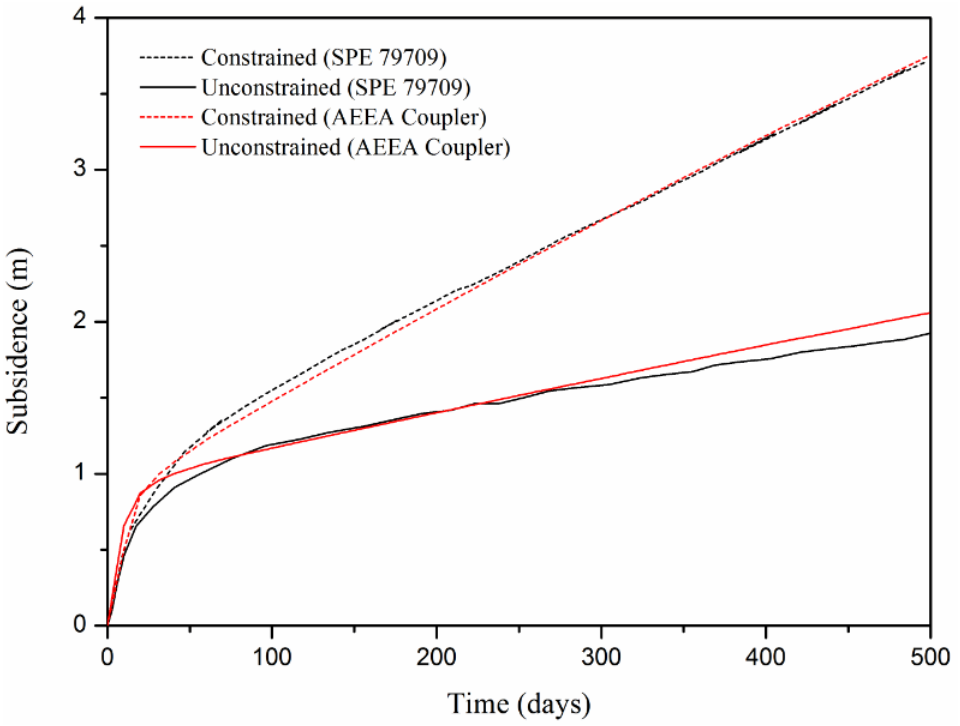

Accepted manuscript
doi: 10.1680/jenge.18.00036

Figure 9. Geometry of the SPE 125760 problem (unit: meter)

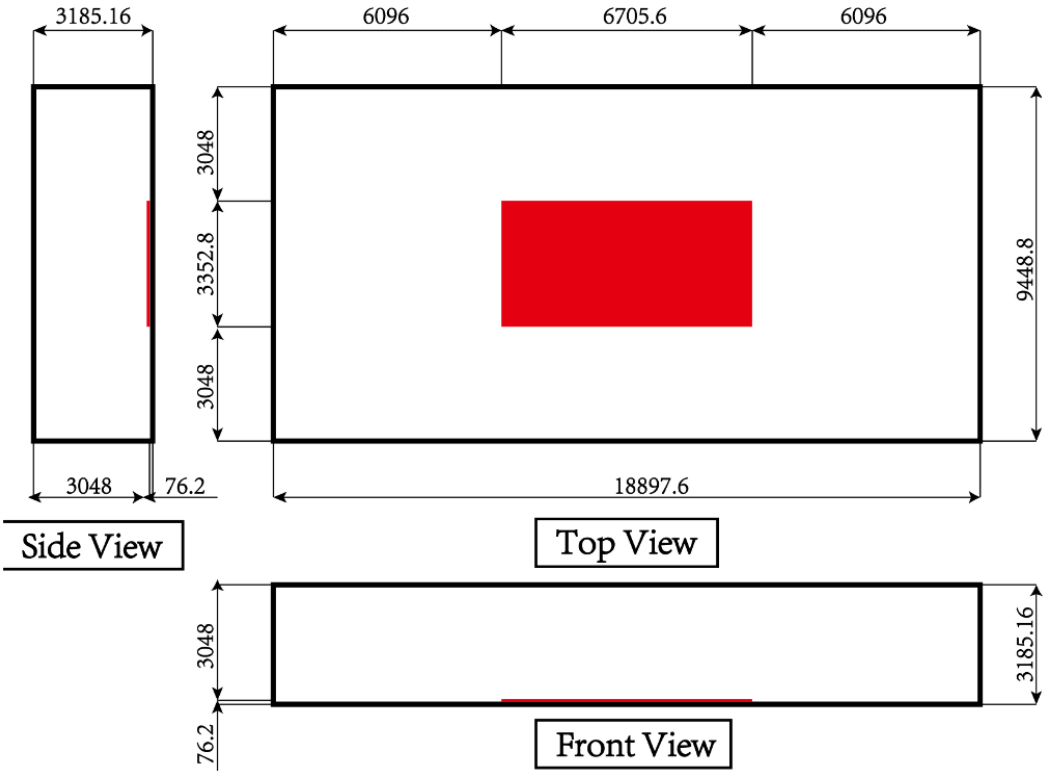

Figure 10. A coarse grid with a discretization of 21×21×12

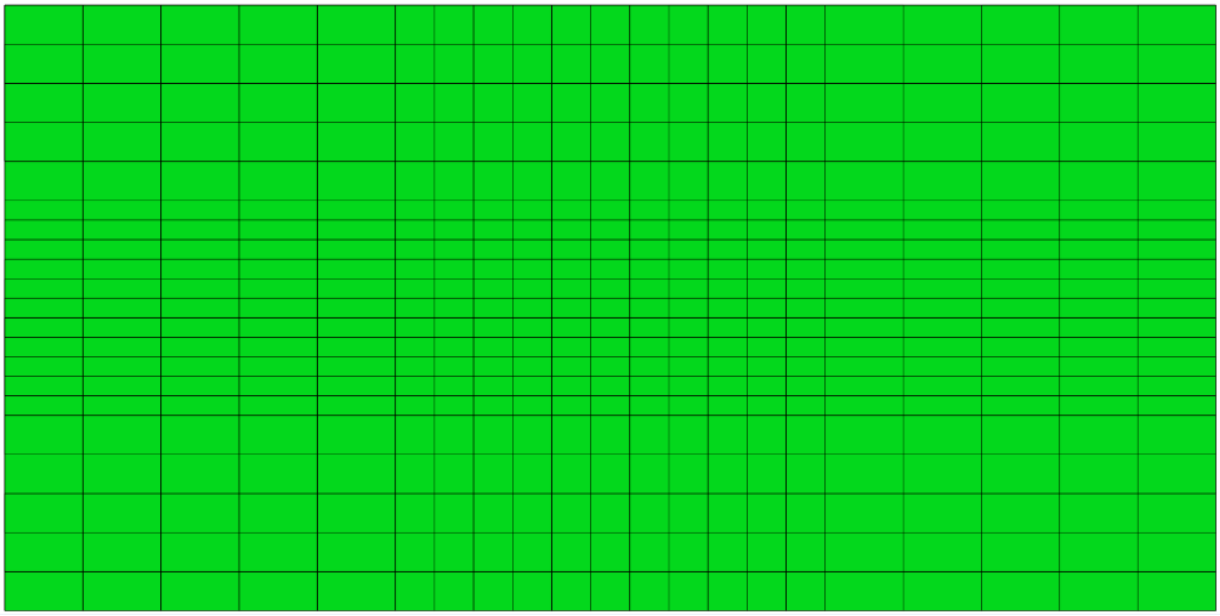

Accepted manuscript
doi: 10.1680/jenge.18.00036

Figure 11. Average pore pressure

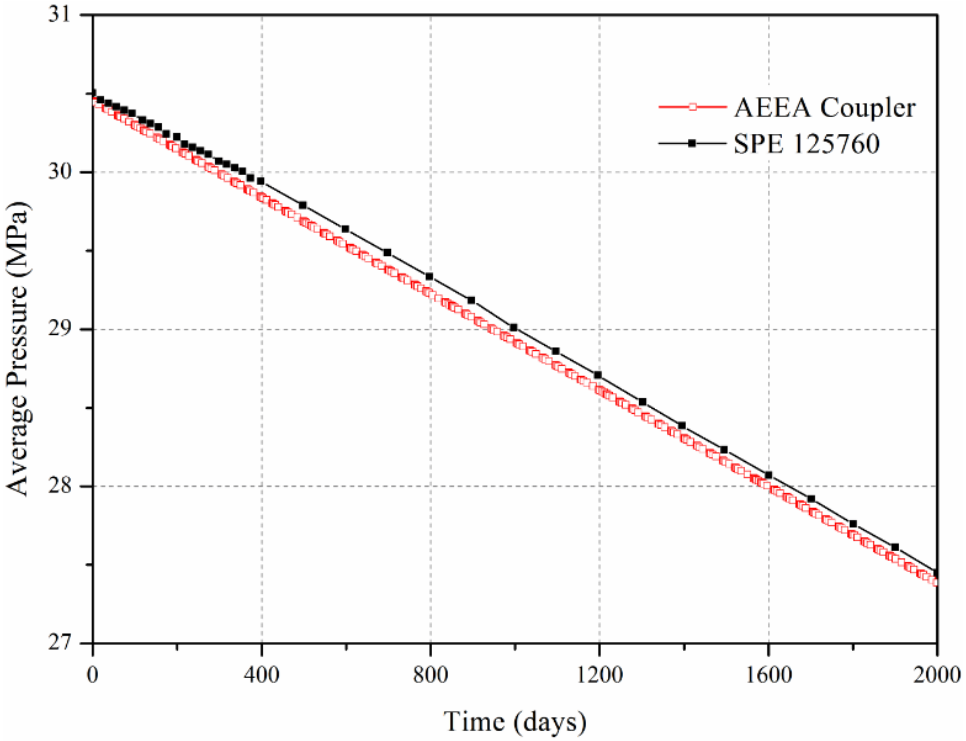

Accepted manuscript
doi: 10.1680/jenge.18.00036

Figure 12. Compaction at the top of the reservoir

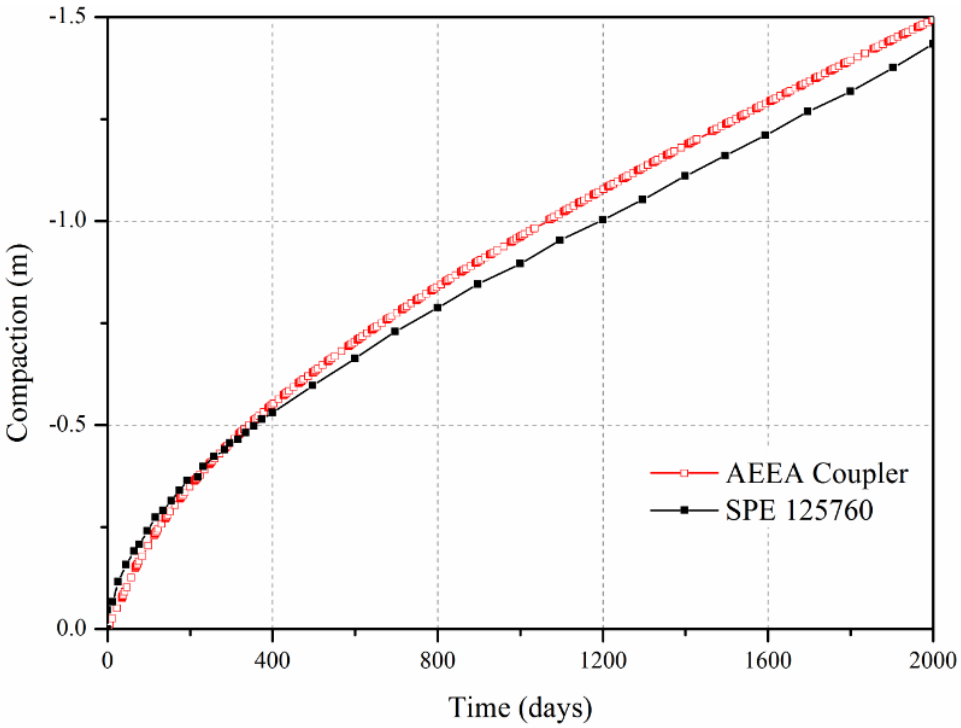

Accepted manuscript
doi: 10.1680/jenge.18.00036

Figure 13. Surface subsidence

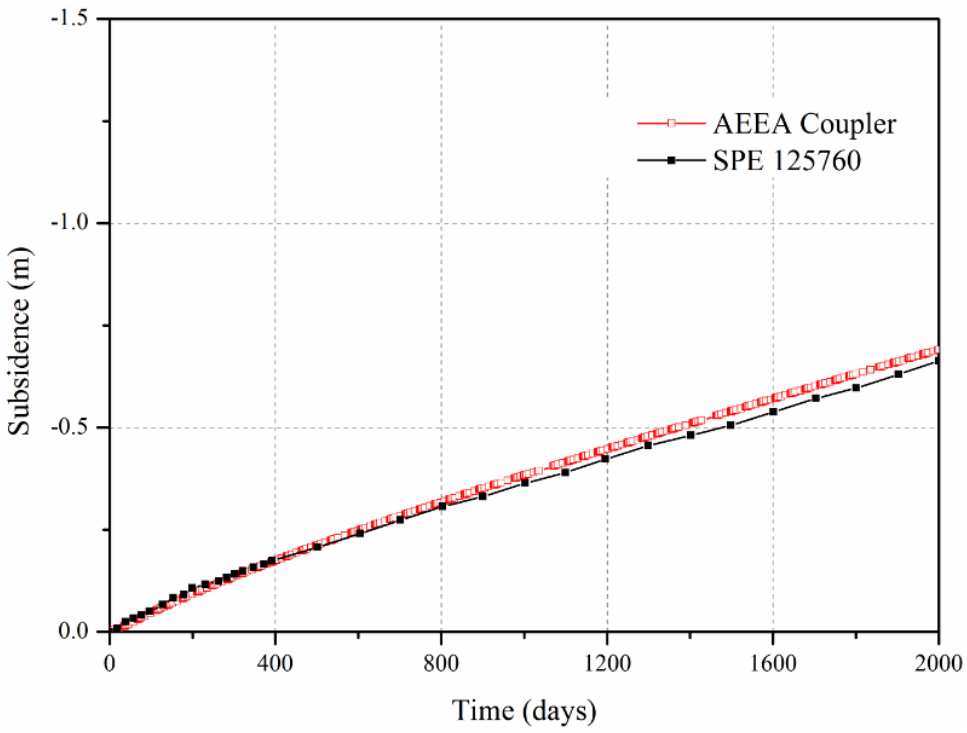

Accepted manuscript
doi: 10.1680/jenge.18.00036

Figure 14. Computational grids

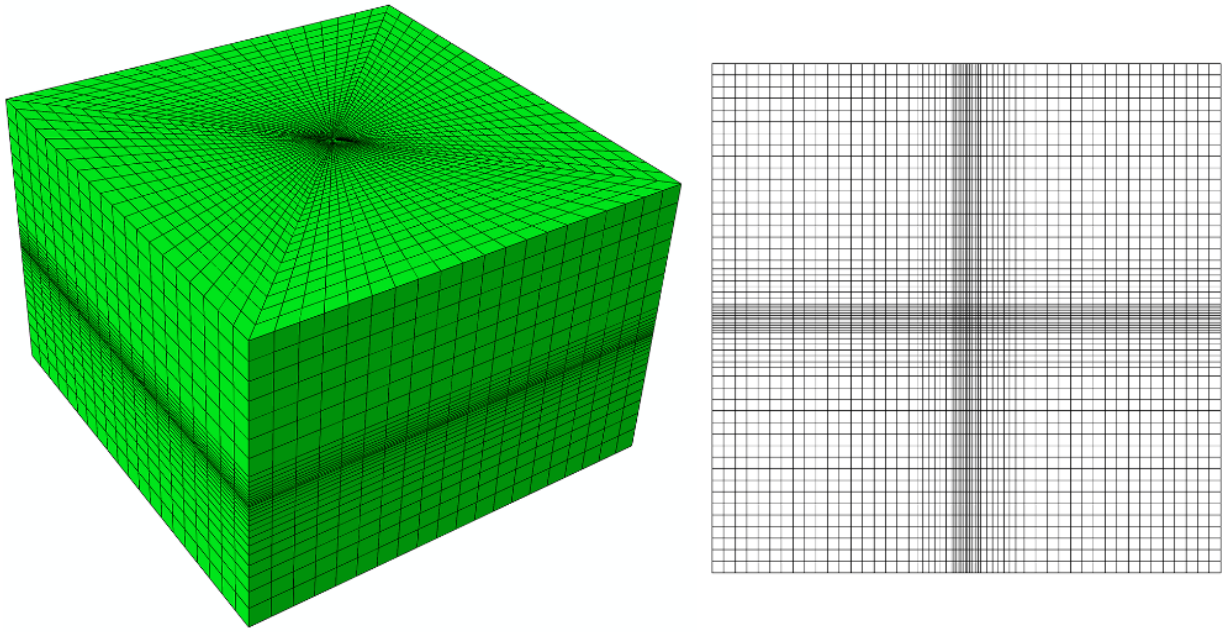

Accepted manuscript
doi: 10.1680/jenge.18.00036

Figure 15. Pore pressure distribution at the top of the reservoir

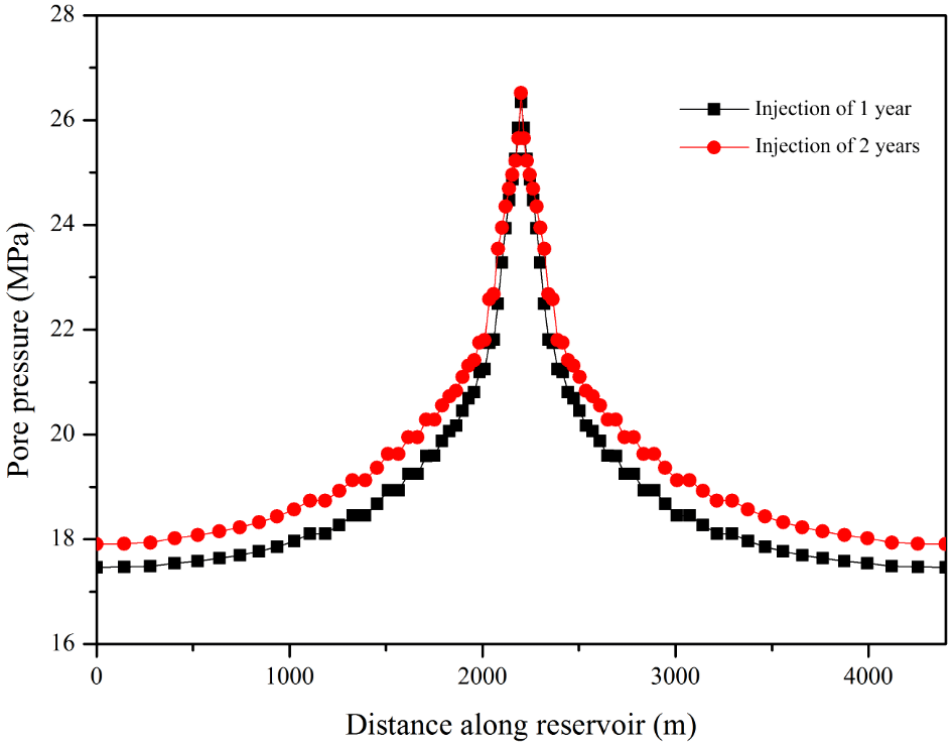

Accepted manuscript
doi: 10.1680/jenge.18.00036

Figure 16. Displacement distribution at the top of the reservoir

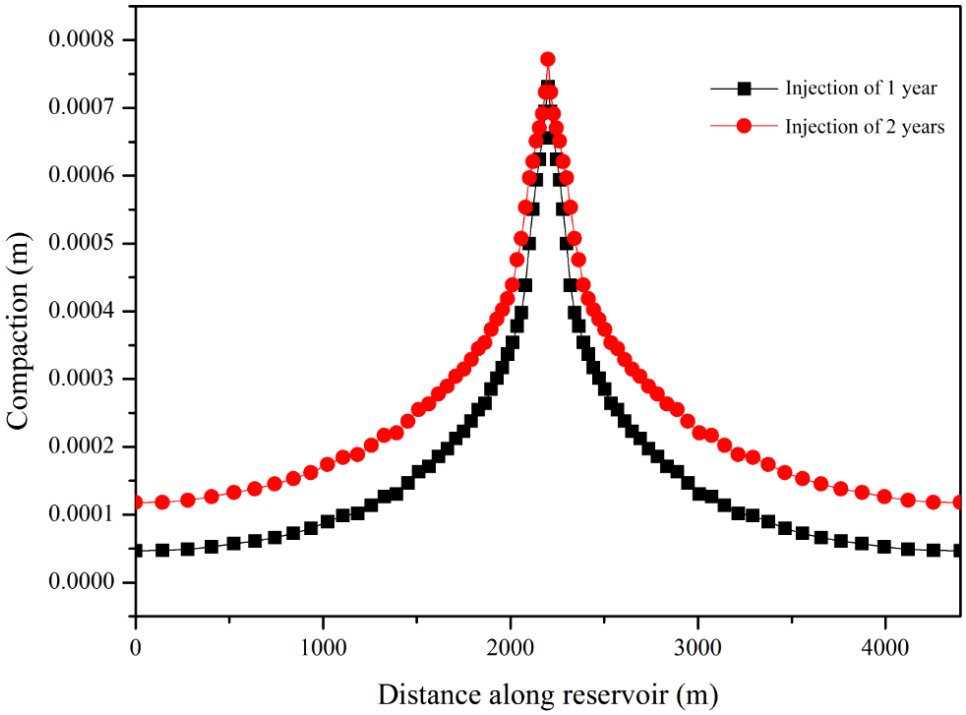

Accepted manuscript
doi: 10.1680/jenge.18.00036

Figure 17. Vertical displacement of the wellbore